

Non-Abelian Dirac oscillator in a uniform Yang–Mills background: spin–isospin mixing and singlet–triplet splitting

Abdelmalek Boumali^{1,*}

ORCID: 0000-0003-2552-0427

¹Laboratory of Theoretical and Applied Physics, Echahid Cheikh Larbi Tebessi University, Algeria

*Corresponding author: boumali.abdelmalek@gmail.com

Abstract

We investigate a planar Dirac oscillator coupled to a spatially uniform $U(2) = U(1) \times SU(2)$ Yang–Mills background. The gauge configuration, adapted from the Dossa–Avossevou construction, contains an Abelian magnetic field B , a non-Abelian spatial amplitude β , and a non-Abelian scalar amplitude ρ . Within the Pauli-reduced formulation, the non-Abelian field strength produces a constant operator on $\mathbb{C}_{\text{spin}}^2 \otimes \mathbb{C}_{\text{iso}}^2$. This operator contains a diagonal internal-Zeeman contribution proportional to $\sigma^3 T^3$ and an off-diagonal spin–isospin term proportional to $\sigma^1 T^1 + \sigma^2 T^2$. Its diagonalization gives a doubly degenerate aligned branch and two mixed branches with eigenvalues

$$\lambda_{\text{FM}} = \frac{g^2 \beta^2}{4m}, \quad \lambda_S = -\frac{g^2 \beta (\beta - 2\rho)}{4m}, \quad \lambda_T = -\frac{g^2 \beta (\beta + 2\rho)}{4m}.$$

Consequently, the aligned internal-Zeeman scale is quadratic in β , whereas the singlet–triplet separation is linear in $\beta\rho$. The revised formulation makes the sign conventions explicit, verifies the main limiting cases, distinguishes the Pauli-reduced spectrum from a full first-order Dirac diagonalization, and clarifies the physical meaning of the numerical illustrations.

Keywords: Dirac oscillator; non-Abelian gauge field; Yang–Mills background; Pauli interaction; spin–isospin coupling; singlet–triplet splitting; graphene bilayers.

1 Introduction

The Dirac oscillator is a paradigmatic exactly solvable relativistic model. It is obtained by introducing a linear non-minimal coupling in the Dirac equation and combines a discrete oscillator-like spectrum with a transparent spin structure [1–3]. Its two-dimensional version is especially useful as an analytical benchmark for graphene-like systems, magnetic confinement, and relativistic quantum simulations [4–8]. In the Abelian case, the oscillator is introduced through

$$\mathbf{p} \longrightarrow \mathbf{p} - im\omega\beta_D \mathbf{r}, \quad (1.1)$$

where m is the mass, ω is the oscillator frequency, and $\beta_D = \gamma^0$.

A natural extension is obtained when the oscillator is coupled to a matrix-valued gauge connection. In a non-Abelian theory, a spatially uniform connection may still generate a nonzero field strength because the Yang–Mills tensor contains the commutator of the gauge potentials. This mechanism has no Abelian analogue and can reorganize the internal degeneracy of the Dirac oscillator. In an earlier aligned construction [9], a single internal generator produced an internal-Zeeman splitting. The purpose of the present work is to analyze the more general

situation in which the background excites several directions of the SU(2) algebra and, as a result, mixes spin and isospin states.

The gauge field used here is the uniform U(2) background introduced by Dossa and Avosevou [10]. It contains an Abelian magnetic sector and a non-Abelian sector governed by two real constants, β and ρ . The parameter β enters the spatial components of the non-Abelian vector potential, while ρ enters the temporal component. Their simultaneous presence generates off-diagonal terms of the form $\sigma^1 T^1 + \sigma^2 T^2$ in the Pauli-reduced operator. These terms resolve the internal sector into aligned and mixed branches and lead to a singlet–triplet splitting proportional to $\beta\rho$.

The paper is organized as follows. Section 2 defines the conventions and evaluates the Yang–Mills field strength. Section 3 derives and diagonalizes the spin–isospin operator. Section 4 presents the Pauli-reduced spectrum, checks the main limits, and discusses the figures. Section 5 summarizes the physical interpretation and states the domain of validity of the result.

2 Model, conventions, and field strength

We use natural units, $\hbar = c = 1$. Greek indices $\mu, \nu = 0, 1, 2$ denote spacetime components, Latin indices $i, j = 1, 2$ denote planar spatial components, and adjoint indices $a, b, c = 1, 2, 3$ label the SU(2) directions. The wave function belongs to

$$\Psi \in \mathbb{C}_{\text{spin}}^2 \otimes \mathbb{C}_{\text{iso}}^2. \quad (2.1)$$

The SU(2) generators are taken in the fundamental representation,

$$T^a = \frac{\tau^a}{2}, \quad [T^a, T^b] = i\epsilon^{abc}T^c, \quad (2.2)$$

where τ^a are Pauli matrices acting in isospin space. The planar Dirac matrices act only on the spinor index. We choose the sign convention in which the Pauli-reduced magnetic spin operator is represented by σ^3 and the aligned limit reproduces the internal-Zeeman scale of Ref. [9].

Following standard non-Abelian gauge-field conventions [11–14], the full U(2) connection is written as

$$\mathcal{A}_\mu = eA_\mu^{(0)}\mathbb{I}_2 + gA_\mu^a T^a, \quad (2.3)$$

with Abelian and non-Abelian coupling constants e and g , respectively. The field strength is

$$\mathcal{F}_{\mu\nu} = eF_{\mu\nu}^{(0)}\mathbb{I}_2 + gF_{\mu\nu}^a T^a, \quad (2.4)$$

where

$$F_{\mu\nu}^{(0)} = \partial_\mu A_\nu^{(0)} - \partial_\nu A_\mu^{(0)}, \quad (2.5)$$

$$F_{\mu\nu}^a = \partial_\mu A_\nu^a - \partial_\nu A_\mu^a - g\epsilon^{abc}A_\mu^b A_\nu^c. \quad (2.6)$$

The last term in Eq. (2.6) is the commutator contribution and remains nonzero for constant non-commuting gauge potentials.

The Abelian sector is chosen in the symmetric gauge,

$$A_0^{(0)} = 0, \quad A_i^{(0)} = -\frac{B}{2}\epsilon_{ij}x_j, \quad (2.7)$$

which gives

$$F_{12}^{(0)} = B, \quad F_{0i}^{(0)} = 0. \quad (2.8)$$

The non-Abelian sector is specified by the Dossa–Avossevou ansatz [10],

$$A_i^a = -\beta\epsilon_{ia}, \quad A_0^a = \rho\delta^{a3}. \quad (2.9)$$

Equivalently, the only nonzero components are

$$A_1^2 = -\beta, \quad A_2^1 = +\beta, \quad A_0^3 = \rho. \quad (2.10)$$

Since β and ρ are constants, the derivative terms in Eq. (2.6) vanish. Direct substitution gives

$$F_{12}^3 = -g\beta^2, \quad (2.11)$$

$$F_{01}^1 = -g\beta\rho, \quad (2.12)$$

$$F_{02}^2 = -g\beta\rho, \quad (2.13)$$

with all other non-Abelian components equal to zero. Thus F_{12}^3 is a commutator-generated non-Abelian magnetic component quadratic in β , whereas F_{01}^1 and F_{02}^2 are electric-type non-Abelian components proportional to $\beta\rho$. For $\rho = 0$, only the diagonal generator T^3 remains. For $\rho \neq 0$, the additional generators T^1 and T^2 are activated and produce spin–isospin mixing.

3 Pauli-reduced spin–isospin operator

In the Pauli-reduced form of the Dirac-oscillator problem, the non-Abelian field strength contributes a constant matrix acting on $\mathbb{C}_{\text{spin}}^2 \otimes \mathbb{C}_{\text{iso}}^2$. With the sign convention stated above, this matrix is

$$\Lambda_{\text{NA}} = \frac{g^2}{2m} [\beta^2 \sigma^3 \otimes T^3 - \beta\rho (\sigma^1 \otimes T^1 + \sigma^2 \otimes T^2)]. \quad (3.1)$$

The first term is diagonal in the σ^3 and T^3 basis and represents the internal-Zeeman contribution. The second term is off-diagonal because it flips spin and isospin simultaneously.

In the ordered basis

$$\{|+, +\rangle, |+, -\rangle, |-, +\rangle, |-, -\rangle\}, \quad (3.2)$$

where the first sign denotes the spin projection and the second sign denotes the isospin projection, Eq. (3.1) becomes

$$\Lambda_{\text{NA}} = \frac{g^2}{4m} \begin{pmatrix} \beta^2 & 0 & 0 & 0 \\ 0 & -\beta^2 & -2\beta\rho & 0 \\ 0 & -2\beta\rho & -\beta^2 & 0 \\ 0 & 0 & 0 & \beta^2 \end{pmatrix}. \quad (3.3)$$

The aligned states $|+, +\rangle$ and $|-, -\rangle$ are eigenstates with the doubly degenerate eigenvalue

$$\lambda_{\text{FM}} = \frac{g^2\beta^2}{4m}. \quad (3.4)$$

The remaining two states are diagonalized by the symmetric and antisymmetric combinations

$$|S\rangle = \frac{1}{\sqrt{2}} (|+, -\rangle - |-, +\rangle), \quad (3.5)$$

$$|T_0\rangle = \frac{1}{\sqrt{2}} (|+, -\rangle + |-, +\rangle), \quad (3.6)$$

with eigenvalues

$$\lambda_S = -\frac{g^2\beta(\beta - 2\rho)}{4m}, \quad (3.7)$$

$$\lambda_T = -\frac{g^2\beta(\beta + 2\rho)}{4m}. \quad (3.8)$$

Here the labels S and T_0 refer to the antisymmetric and symmetric spin–isospin combinations in Eq. (3.5)–(3.6); they should not be interpreted as an exactly degenerate $SU(2)$ multiplet of the full anisotropic operator.

The resulting mixed-branch separation is

$$\Delta\lambda_{ST} = \lambda_S - \lambda_T = \frac{g^2\beta\rho}{m}. \quad (3.9)$$

This is the central mathematical result. The aligned internal-Zeeman effect is quadratic in β , while the singlet–triplet splitting is linear in the product $\beta\rho$.

4 Spectrum, limiting checks, and numerical illustration

The Abelian magnetic field and the Dirac-oscillator coupling combine into the effective scale

$$\Omega_{\text{eff}} = m\omega + \frac{eB}{2}. \quad (4.1)$$

The corresponding planar magnetic Dirac-oscillator backbone is

$$\left(E_{n,s}^{(0)}\right)^2 = m^2 + 2\Omega_{\text{eff}}(2n + 1 - s), \quad n = 0, 1, 2, \dots, \quad s = \pm 1. \quad (4.2)$$

Within the factorized Pauli-reduced spectral problem, the internal eigenvalues of Eq. (3.1) enter as additive mass-squared shifts:

$$E_{n,s,k}^{(\pm)} = \pm\sqrt{m^2 + 2\Omega_{\text{eff}}(2n + 1 - s) + 2m\lambda_k}, \quad k \in \{\text{FM}, S, T\}. \quad (4.3)$$

The radicand must be non-negative. This condition is automatically satisfied in the weak-field regime but can restrict the triplet branch when $\beta\rho > 0$ is sufficiently large.

The standard limits are recovered consistently. If $\beta = \rho = B = 0$, Eq. (4.3) reduces to the planar Dirac-oscillator spectrum

$$E_{n,s}^{(\pm)} = \pm\sqrt{m^2 + 2m\omega(2n + 1 - s)}. \quad (4.4)$$

If $\beta = \rho = \omega = 0$, one obtains the relativistic Landau-type spectrum in $(2 + 1)$ dimensions,

$$E_{n,s}^{(\pm)} = \pm\sqrt{m^2 + eB(2n + 1 - s)}. \quad (4.5)$$

For $\beta = \rho = 0$, the non-Abelian sector decouples and the magnetic field shifts the oscillator scale according to Eq. (4.1), in agreement with the magnetic Dirac-oscillator interpretation of Refs. [7, 8].

The aligned non-Abelian limit is obtained by setting $\rho = 0$. Then

$$\lambda_S = \lambda_T = -\frac{g^2\beta^2}{4m}, \quad \lambda_{\text{FM}} = +\frac{g^2\beta^2}{4m}, \quad (4.6)$$

so the internal separation is

$$\lambda_{\text{FM}} - \lambda_{S,T} = \frac{g^2\beta^2}{2m} \equiv \zeta. \quad (4.7)$$

Equation (4.7) reproduces the internal-Zeeman scale used in the aligned construction. However, Eq. (4.3) is a square-root spectrum of the Pauli-reduced second-order operator, whereas the aligned result of Ref. [9] was written as a first-order channel shift. The consistent weak-background comparison is therefore

$$E_{n,s,k}^{(+)} = E_{n,s}^{(0)} + \frac{m\lambda_k}{E_{n,s}^{(0)}} + \mathcal{O}(\lambda_k^2), \quad (4.8)$$

which gives

$$E_{n,s,\text{FM}}^{(+)} - E_{n,s,S/T}^{(+)} = \frac{m\zeta}{E_{n,s}^{(0)}} + \mathcal{O}(\zeta^2). \quad (4.9)$$

For $\rho \neq 0$, the exact positive-energy singlet–triplet difference is

$$\Delta E_{ST}^{(+)} = \sqrt{\left(E_{n,s}^{(0)}\right)^2 + 2m\lambda_S} - \sqrt{\left(E_{n,s}^{(0)}\right)^2 + 2m\lambda_T}, \quad (4.10)$$

and its weak-field form is

$$\Delta E_{ST}^{(+)} \simeq \frac{m(\lambda_S - \lambda_T)}{E_{n,s}^{(0)}} = \frac{g^2 \beta \rho}{E_{n,s}^{(0)}}. \quad (4.11)$$

Thus the leading observable separation is linear in $\beta\rho$ and suppressed by the relativistic backbone energy.

Figures 1–4 illustrate the analytical formulas in normalized units $g = m = e = 1$, with $B = 0.5$ and $\omega = 0.5$ unless otherwise indicated. These figures are not fitted to a specific material; they are intended to display the spectral mechanisms implied by Eqs. (3.4)–(4.3).

Figure 1 shows the spectrum as a function of β . In the aligned case $\rho = 0$, the internal sector has two distinct levels: the doubly degenerate aligned branch and the degenerate mixed branch. For $\rho = 0.4$, the off-diagonal spin–isospin coupling separates the mixed branches. Figure 2 shows the positive-energy branches as functions of ρ at fixed $\beta = 0.5$: the aligned branch is independent of ρ , while the S and T branches move in opposite directions. Figure 3 plots the internal eigenvalues directly and therefore isolates the algebraic origin of the splitting. Finally, Fig. 4 checks the aligned limit by comparing the exact Pauli-reduced square-root branches with the leading expansion in Eq. (4.8).

Extended non-Abelian Dirac oscillator: $B=0.5, \omega=0.5, g=m=1$

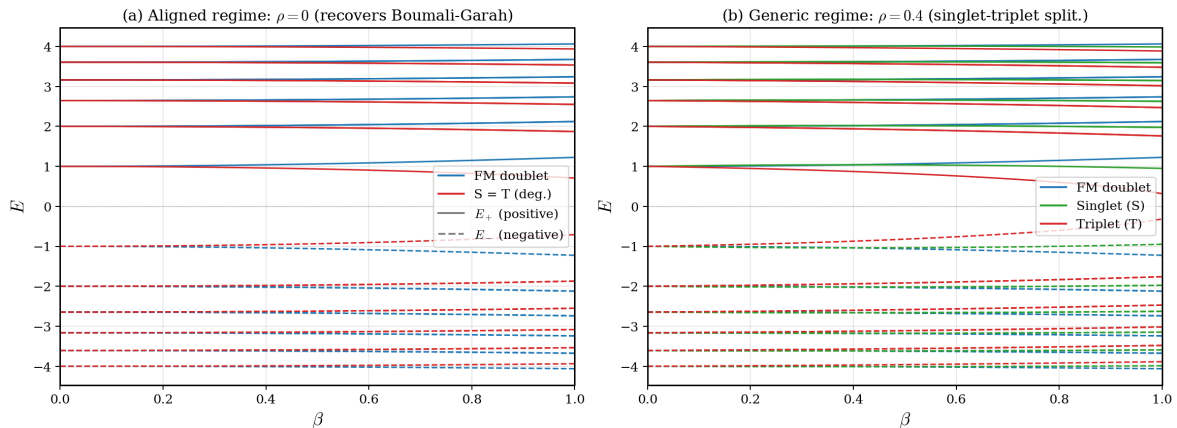


Figure 1: Spectrum as a function of the non-Abelian vector amplitude β . Panel (a): aligned case $\rho = 0$, with an aligned doublet and a degenerate mixed branch. Panel (b): generic case $\rho = 0.4$, where the scalar non-Abelian component activates the off-diagonal spin–isospin coupling and separates the S and T branches. Solid lines denote positive-energy states and dashed lines denote negative-energy states.

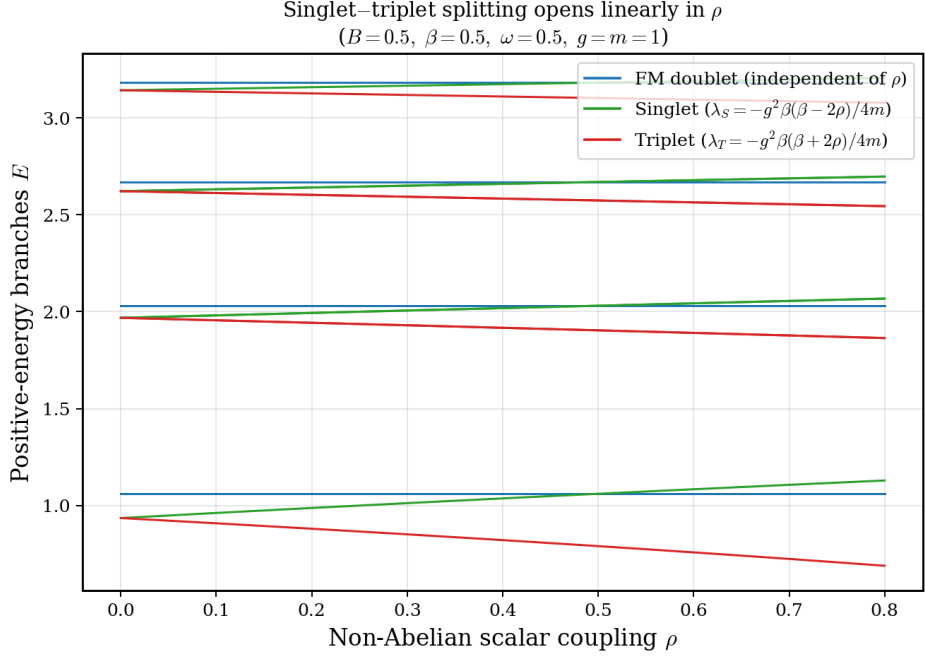


Figure 2: Positive-energy branches as functions of the scalar non-Abelian amplitude ρ at fixed $\beta = 0.5$. The aligned branch is independent of ρ , whereas the mixed branches separate linearly at leading order, as described by Eq. (4.11).

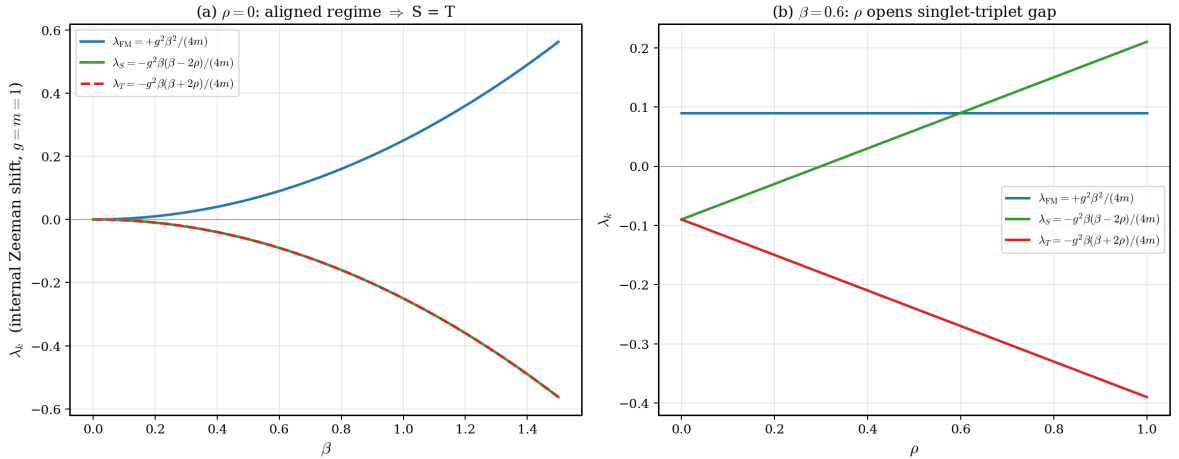


Figure 3: Internal eigenvalues λ_k of the spin–isospin matrix Λ_{NA} . Panel (a): for $\rho = 0$, the aligned branch grows as $+\beta^2$, while the two mixed branches coincide and decrease as $-\beta^2$. Panel (b): for fixed $\beta = 0.6$, the aligned eigenvalue is constant while λ_S and λ_T separate linearly in ρ .

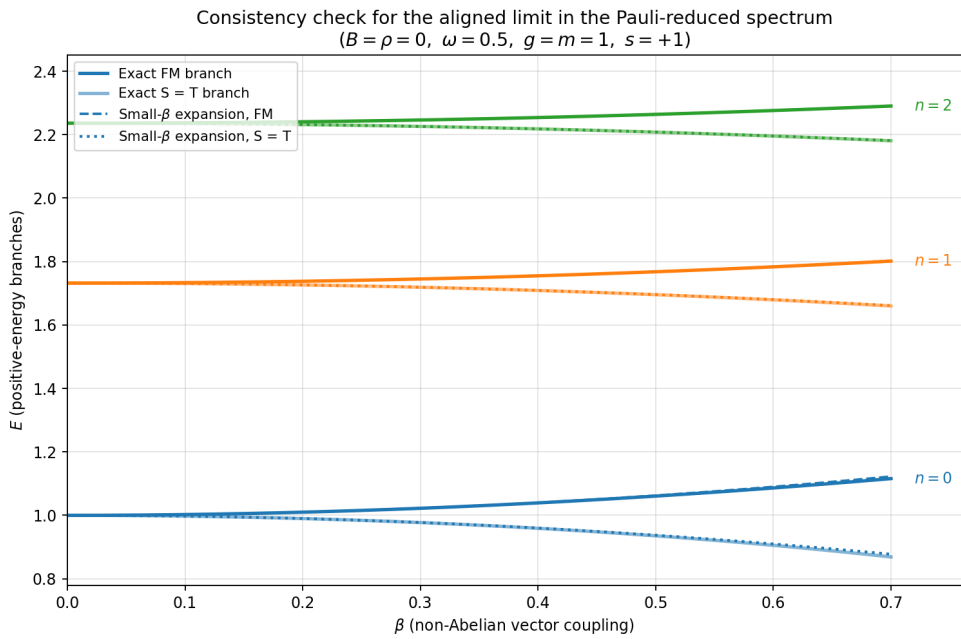


Figure 4: Consistency check of the aligned limit $\rho = 0$. Solid curves are the exact positive-energy branches of the Pauli-reduced square-root spectrum for $n = 0, 1, 2$. Dashed and dotted curves show the leading small- β expansion of Eq. (4.8). The agreement confirms the perturbative interpretation of the aligned comparison.

5 Discussion and conclusion

The extended Yang–Mills background converts a purely diagonal internal-Zeeman problem into a mixed spin–isospin problem. In the aligned limit, the non-Abelian connection selects the generator T^3 , and the internal sector separates into two independent branches. When $\rho \neq 0$, the temporal component of the connection does not commute with the spatial components. The commutator part of the field strength then generates the operators $\sigma^1 T^1$ and $\sigma^2 T^2$, which couple $|+, -\rangle$ and $|-, +\rangle$ and produce the mixed states in Eqs. (3.5) and (3.6).

This structure is relevant as an analytically solvable benchmark for systems with matrix-valued gauge potentials. In bilayer graphene, for example, layer or sublattice degrees of freedom may play the role of an internal pseudospin, and effective non-Abelian gauge potentials can arise from interlayer coupling or strain-related mechanisms [15–18]. Similar ideas also appear in cold-atom realizations of synthetic non-Abelian gauge fields [19, 20]. The present model should not be read as a microscopic description of a particular device; rather, it identifies the algebraic mechanism by which a uniform matrix-valued background splits internal branches.

The scope of Eq. (4.3) should also be emphasized. It is the spectrum of the factorized Pauli-reduced operator. If one starts instead from a fully first-order Dirac Hamiltonian with non-commuting spin-dependent potentials, the full spinor–orbital Hamiltonian must be diagonalized directly or treated perturbatively. The present result is therefore a controlled Pauli-reduced spectral model and a diagnostic of the splitting generated by the Yang–Mills commutator.

In summary, the non-Abelian Dirac oscillator in the uniform $U(2)$ background possesses one aligned internal branch and two mixed branches. The aligned internal-Zeeman scale is $\zeta = g^2 \beta^2 / (2m)$, while the mixed-branch splitting is $\Delta\lambda_{ST} = g^2 \beta \rho / m$. The latter is absent in the purely aligned model and provides the characteristic signature of the off-diagonal Yang–Mills components. Natural extensions include higher isospin representations, non-uniform backgrounds $\beta(\mathbf{x})$ and $\rho(\mathbf{x})$, and microscopic realizations in graphene-inspired or cold-atom platforms.

References

- [1] M. Moshinsky and A. Szczepaniak, “The Dirac oscillator,” *Journal of Physics A: Mathematical and General* **22**, L817–L819 (1989), doi:[10.1088/0305-4470/22/17/002](https://doi.org/10.1088/0305-4470/22/17/002).
- [2] J. Benítez, R. P. Martínez-y-Romero, H. N. Núñez-Yépez, and A. L. Salas-Brito, “Solution and hidden supersymmetry of a Dirac oscillator,” *Physical Review Letters* **64**, 1643–1645 (1990), doi:[10.1103/PhysRevLett.64.1643](https://doi.org/10.1103/PhysRevLett.64.1643).
- [3] R. Jagannathan, “A two-component Dirac oscillator with anomalous magnetic interaction,” *Physical Review A* **42**, 6674–6676 (1990), doi:[10.1103/PhysRevA.42.6674](https://doi.org/10.1103/PhysRevA.42.6674).
- [4] A. Bermúdez, M. A. Martín-Delgado, and A. Luis, “Exact solution of the (2+1)-dimensional Dirac oscillator,” *Physical Review A* **77**, 063815 (2008), doi:[10.1103/PhysRevA.77.063815](https://doi.org/10.1103/PhysRevA.77.063815).
- [5] R. Gerritsma, G. Kirchmair, F. Zähringer, E. Solano, R. Blatt, and C. F. Roos, “Quantum simulation of the Dirac equation,” *Nature* **463**, 68–71 (2010), doi:[10.1038/nature08688](https://doi.org/10.1038/nature08688).
- [6] J. A. Franco-Villafañe, E. Sadurní, S. Barkhofen, U. Kuhl, F. Mortessagne, and T. H. Seligman, “First experimental realization of the Dirac oscillator,” *Physical Review Letters* **111**, 170405 (2013), doi:[10.1103/PhysRevLett.111.170405](https://doi.org/10.1103/PhysRevLett.111.170405).
- [7] A. Boumali, “The relativistic Dirac oscillator in a magnetic field,” *Physica Scripta* **90**, 045702 (2015), doi:[10.1088/0031-8949/90/4/045702](https://doi.org/10.1088/0031-8949/90/4/045702).

- [8] A. Belouad, A. Jellal, and Y. Zahidi, “Gate-tunable graphene quantum dot and Dirac oscillator,” *Physics Letters A* **380**, 773–778 (2016), doi:[10.1016/j.physleta.2015.11.025](https://doi.org/10.1016/j.physleta.2015.11.025).
- [9] A. Boumali and S. Garah, “Non-Abelian extensions of the Dirac oscillator: A theoretical approach,” *Modern Physics Letters A* (2026); arXiv:2504.08978.
- [10] F. A. Dossa and G. Y. H. Avossevou, “Relativistic dynamics for a particle carrying a non-Abelian charge in a non-Abelian background electromagnetic field,” *Journal of Mathematical Physics* **61**, 022302 (2020), doi:[10.1063/1.5123595](https://doi.org/10.1063/1.5123595).
- [11] C. N. Yang and R. L. Mills, “Conservation of isotopic spin and isotopic gauge invariance,” *Physical Review* **96**, 191–195 (1954), doi:[10.1103/PhysRev.96.191](https://doi.org/10.1103/PhysRev.96.191).
- [12] S. K. Wong, “Field and particle equations for the classical Yang-Mills field and particles with isotopic spin,” *Il Nuovo Cimento A* **65**, 689–694 (1970), doi:[10.1007/BF02892134](https://doi.org/10.1007/BF02892134).
- [13] L. H. Ryder, *Quantum Field Theory*, 2nd ed. (Cambridge University Press, Cambridge, 1996).
- [14] J. Fröhlich and U. M. Studer, “Gauge invariance and current algebra in non-relativistic many-body theory,” *Reviews of Modern Physics* **65**, 733–802 (1993), doi:[10.1103/RevModPhys.65.733](https://doi.org/10.1103/RevModPhys.65.733).
- [15] A. H. Castro Neto, F. Guinea, N. M. R. Peres, K. S. Novoselov, and A. K. Geim, “The electronic properties of graphene,” *Reviews of Modern Physics* **81**, 109–162 (2009), doi:[10.1103/RevModPhys.81.109](https://doi.org/10.1103/RevModPhys.81.109).
- [16] M. A. H. Vozmediano, M. I. Katsnelson, and F. Guinea, “Gauge fields in graphene,” *Physics Reports* **496**, 109–148 (2010), doi:[10.1016/j.physrep.2010.07.003](https://doi.org/10.1016/j.physrep.2010.07.003).
- [17] P. San-Jose, J. González, and F. Guinea, “Non-Abelian gauge potentials in graphene bilayers,” *Physical Review Letters* **108**, 216802 (2012), doi:[10.1103/PhysRevLett.108.216802](https://doi.org/10.1103/PhysRevLett.108.216802).
- [18] A. Ramires and J. L. Lado, “Electrically tunable gauge fields in tiny-angle twisted bilayer graphene,” *Physical Review Letters* **121**, 146801 (2018), doi:[10.1103/PhysRevLett.121.146801](https://doi.org/10.1103/PhysRevLett.121.146801).
- [19] J. Dalibard, F. Gerbier, G. Juzeliūnas, and P. Öhberg, “Colloquium: Artificial gauge potentials for neutral atoms,” *Reviews of Modern Physics* **83**, 1523–1543 (2011), doi:[10.1103/RevModPhys.83.1523](https://doi.org/10.1103/RevModPhys.83.1523).
- [20] N. Goldman, G. Juzeliūnas, P. Öhberg, and I. B. Spielman, “Light-induced gauge fields for ultracold atoms,” *Reports on Progress in Physics* **77**, 126401 (2014), doi:[10.1088/0034-4885/77/12/126401](https://doi.org/10.1088/0034-4885/77/12/126401).